

A gigantic intraosseous and dural-based calvarial metastatic follicular thyroid carcinoma: illustrative case

Anthony T. Lee, MD, PhD,¹ Kunal P. Raygor, MD,² Noah M. Nichols, MD,³ and Phiroz E. Tarapore, MD^{1,4}

¹Department of Neurological Surgery, University of California, San Francisco, San Francisco, California; ²Department of Neurosurgery, Vanderbilt University Medical Center, Nashville, Tennessee; ³Department of Neurosurgery, Mount Sinai Health System, New York, New York; and ⁴Brain and Spinal Injury Center, San Francisco General Hospital, San Francisco, California

BACKGROUND Metastatic follicular thyroid carcinoma to the central nervous system (CNS), including the skull and dura, is exceedingly rare.

OBSERVATIONS The authors present the case of a gigantic, intraosseous, dural-based follicular thyroid carcinoma, highlighting the operative strategy for this mass. They also provide a literature review of CNS metastases of differentiated thyroid carcinoma.

LESSONS Although follicular thyroid carcinoma rarely metastasizes to the CNS, it should be included in the differential diagnosis of hypervascular intraosseous skull lesions, even in the absence of disseminated metastatic disease. The authors illustrate key operative steps in managing the tumor's hypervascularity, extracranial extension, and posterior sagittal sinus invasion, as well as unintended sequelae from ligating the seemingly occluded anterior and middle third of the superior sagittal sinus in large tumors.

<https://thejns.org/doi/abs/10.3171/CASE24550>

KEYWORDS metastatic thyroid carcinoma; follicular thyroid carcinoma; transcalvarial; gigantic

Metastatic follicular thyroid carcinoma to the calvaria and dura is rare and has only been described in limited case series in the literature. The surgical management of a gigantic, metastatic, transcalvarial, dural-based follicular thyroid carcinoma has not been extensively reported. In this study, we describe the case of a large, dural-based, metastatic follicular thyroid carcinoma with calvarial invasion and exophytic extracranial growth. We conclude with a discussion of the literature regarding metastatic thyroid carcinoma in the central nervous system (CNS).

Illustrative Case

A 63-year-old woman with a history of schizophrenia presented with a 2-year history of neck pain and a rapidly expanding mass lesion on the top of her cranium (Fig. 1A). Magnetic resonance imaging/magnetic resonance venography (MRI/MRV) of the brain showed a large, 14 × 12 × 11-cm (anteroposterior × transverse × craniocaudal), extra-axial, transdiploic, hypervascular mass with internal hemorrhage, associated with invasion into the superior sagittal sinus (SSS) and multifocal sulcal effacement in the left frontal and bilateral parietal lobes with a 1.3-cm midline shift and uncal herniation (Fig. 1B and C).

A computed tomography (CT) scan for primary malignancy revealed a single left thyroid calcification. Her neurological examination revealed no focal deficits. Because of the massive size of the lesion and rate of expansion, the patient elected to proceed with resection.

Because of the hypervascularity of the lesion, a cerebral angiogram with embolization was obtained prior to surgery, which demonstrated bilateral vascular supply (Fig. 2). The mass was supplied by the right anterior meningeal artery and left middle cerebral and ophthalmic arteries, and there was bilateral supply via occipital, superficial temporal, and middle meningeal arteries (Fig. 2B). The middle third of the SSS was found to be occluded (Fig. 2C; venous phase digital subtraction angiography). Significant blood supply remained via the bilateral occipital and superficial temporal arteries following embolization of the bilateral middle meningeal arteries (Fig. 2D).

In the operating room, a biparietal-occipital craniotomy with plastic surgery mesh cranioplasty was performed. The scalp incision was extended from tragus to tragus (Fig. 3A and B), and the scalp flap was reflected both anteriorly and posteriorly. The plane between the galea and tumor was developed 360° around the tumor, and the dissection was carried forward until the bone of the calvaria was identified entirely

ABBREVIATIONS CNS=central nervous system; CT=computed tomography; DTC=differentiated thyroid carcinoma; HR=hazard ratio; IPH=intraparenchymal hemorrhage; MRI=magnetic resonance imaging; MRV=magnetic resonance venography; SSS=superior sagittal sinus.

INCLUDE WHEN CITING Published December 16, 2024; DOI: 10.3171/CASE24550.

SUBMITTED August 19, 2024. **ACCEPTED** October 14, 2024.

© 2024 The authors, CC BY-NC-ND 4.0 (<http://creativecommons.org/licenses/by-nc-nd/4.0/>)

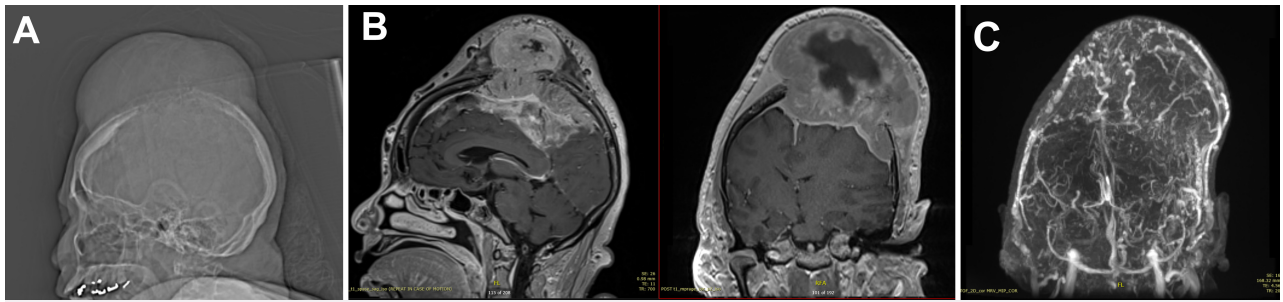


FIG. 1. Preoperative MRI/MRV. **A:** Scout image showing a large calvarial mass arising from the vertex. **B:** Sagittal and coronal postcontrast T1-weighted MRI showing a 14 × 12 × 11-cm, extra-axial, transdiploic mass with internal hemorrhage, associated invasion into the SSS, and sulcal effacement of left frontal and bilateral parietal lobes with 1.3 cm of midline shift and uncus herniation. **C:** Coronal MRV showing a hypervascular mass.

around the perimeter of the tumor (Fig. 3C). Following completion of the scalp dissection, the extracranial portion of the tumor was then removed. The tumor was dissected off the bone until it became clear that the central portion of the tumor had completely invaded and lysed all the bone. At that point, the tumor was centrally debulked and a large cystic space within the center of the tumor filled with dark motor oil-colored fluid was entered. This was found to represent an area of old hemorrhage within the tumor itself. Following debulking, the tumor was easier to manipulate and was subsequently amputated in the plane of the calvaria.

To address the intracranial portion of the tumor, a piecemeal circumferential craniotomy was fashioned to reveal normal dura surrounding the lesion. First, a burr hole was drilled at the anterior portion of the tumor, just lateral to the sagittal sinus (Fig. 3D). Another burr hole was drilled in the right frontal region. A small craniotomy was fashioned between the 12- and 3-o'clock positions of the tumor, removing the right frontal portion of the bone surrounding the tumor.

The medial portion of the bone flap was completely eroded and was subsequently lifted off the tumor. The same technique was used to remove the bone in 3 additional sections. The second section went from the 3- to 6-o'clock position, just lateral to the sagittal sinus. The third section went from the 6- to 9-o'clock position over the sagittal sinus, after carefully dissecting the dura off the underside of the bone. The final section of bone was elevated off the sagittal sinus. At this point, the dura had been exposed 360° around the tumor.

Having completed the craniotomy, we turned our attention toward the intradural portion of the tumor. The dura was opened on either side of the tumor margin, and the dura was reflected medially toward the center of the tumor. A clear plane was identified between the tumor and the underlying cortex (Fig. 3E). There was, in fact, no significant attachment between the tumor itself and the cortex, so after significant central debulking of the tumor, it became possible to lift the rim of the tumor up and off the cortical boundary and reflect it medially toward the SSS.

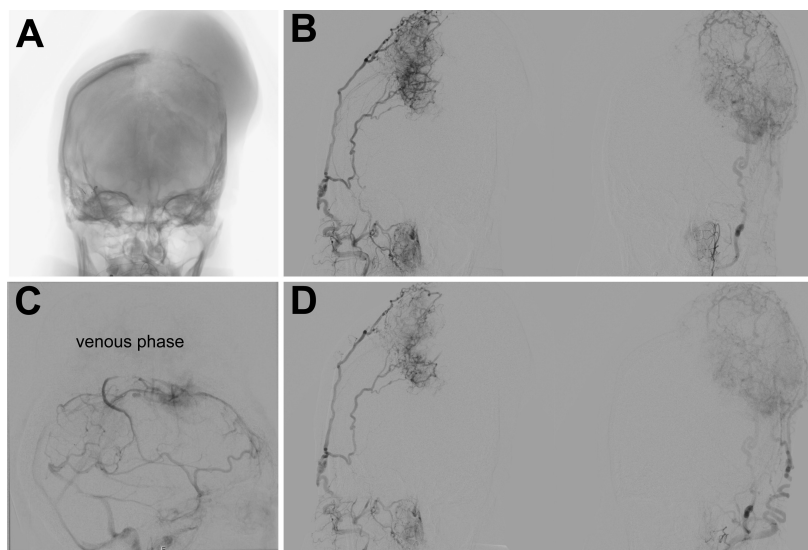


FIG. 2. Preoperative angiograms. **A:** Anteroposterior projection showing the location of a large calvarial mass. **B:** Coronal projection showing extensive bilateral external carotid artery supply. **C:** Lateral angiogram showing occlusion of the middle third of SSS in the venous phase. **D:** Significant blood supply remained following bilateral embolization of the middle meningeal arteries.

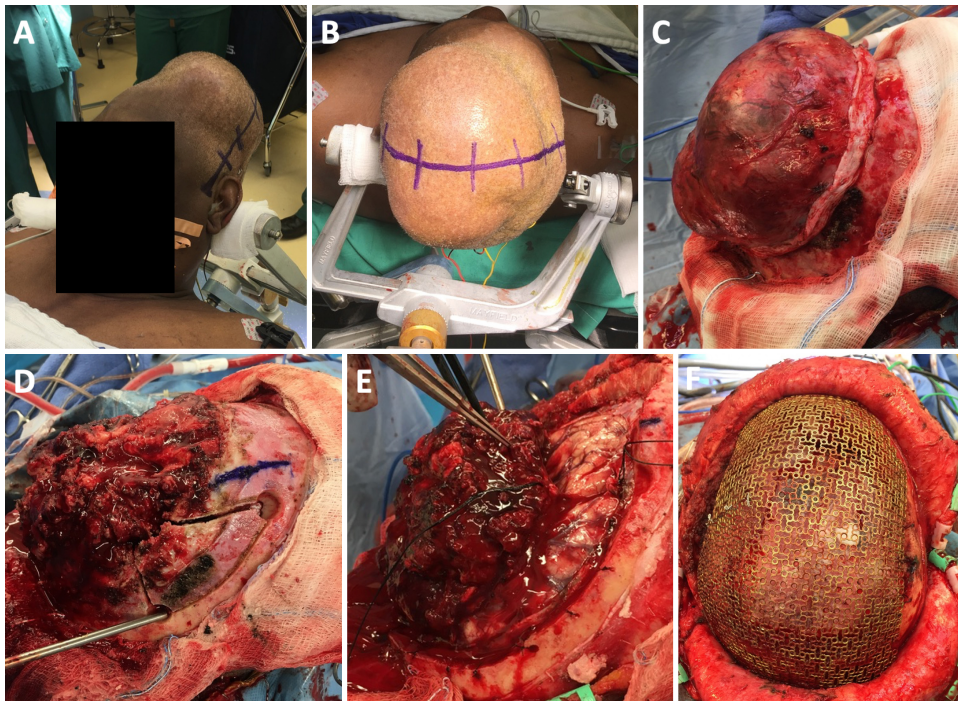


FIG. 3. Intraoperative photographs of biparietal-occipital craniotomy with plastic surgery mesh cranioplasty. **A and B:** The scalp incision was extended from tragus to tragus. **C:** Circumferential dissection of the galea from the tumor. **D:** Placement of burr holes. **E:** Identification of plane between the tumor and underlying cortex. **F:** Mesh reconstruction of the 40 × 40-cm cranial defect.

Subsequently, the tumor was dissected off the SSS. The anterior portion of the sinus was entered and found to have minimal flow. It was suture ligated on either side, and the falx was divided and elevated out of the interhemispheric fissure. The tumor came easily off the cortical layer. As the dissection advanced posteriorly, it became clear that both the left and right veins of Trolard were traveling within the dura of the tumor itself before inserting into the sagittal sinus and reconstituting the sinus posterior to the tumor. The decision was made to preserve these 2 venous attachments to avoid causing a significant venous infarct in the patient's primary motor cortex. The ultrasonic aspiration device was therefore used to debride all gross tumor from the dural surface anterior to the remaining 10% of tumor overlying the vein of Trolard. Of note, the patient did have monopolar mapping of both motor strips throughout the case, and the motor system was found to be intact and stimulating at normal physiological thresholds.

Having achieved a maximal, safe, radical subtotal resection of the tumor, we decided to close the incision. The plastic surgery team was consulted for reconstruction of the 40 × 40-cm cranial defect (Fig. 3F).

The patient's postoperative course was complicated. She experienced a grand mal, tonic-clonic seizure after closure but prior to extubation and was kept intubated in the intensive care unit thereafter. Neurologically, the patient was comatose for 2 weeks after surgery. Postoperative head CT and MRI showed evolving left occipital and right frontal intraparenchymal hemorrhage (IPH), along with cerebral edema secondary to venous congestion (Fig. 4A and B). A micro-sensor was placed, which showed low intracranial pressures, and a video electroencephalogram revealed no evidence of epileptiform

activity. During this period, the patient developed ventilator-associated pneumonia. A repeat CT/CT angiography study on postoperative day 4 demonstrated improving cerebral edema and stable venous flow compared to the patient's preoperative condition. A subsequent repeat angiogram (Fig. 4C) showed that the posterior third of the SSS remained patent, with unchanged dural venous sinuses and deep cerebral veins. Three weeks later, a combined thyroidectomy and tracheostomy was performed by the otolaryngology team, and a percutaneous endoscopic gastrostomy was subsequently placed by interventional radiology. Slowly, the patient emerged from coma and became progressively more alert and oriented. She was able to follow commands and move her right side with antigravity strength but remained plegic on the left. The patient was discharged to a skilled nursing facility.

Five months after surgery, the patient returned with progressive communicating hydrocephalus, which was managed with the placement of a ventriculoperitoneal shunt. Follow-up imaging showed the expected radical subtotal resection (Fig. 4D). At the 20-month follow-up, her modified Rankin Scale score was 4: she was alert and oriented to person, place, and date, following commands with her right upper extremity, with minimal movement of her left upper extremity, and wiggling her toes bilaterally. Her left hemiparesis continued to improve, and at the 4-year follow-up, the patient was doing well with antigravity movement in all extremities.

Pathology

Morphological profiling demonstrated sheets of glands and follicles of varying sizes filled with colloid, resembling thyroid parenchyma.

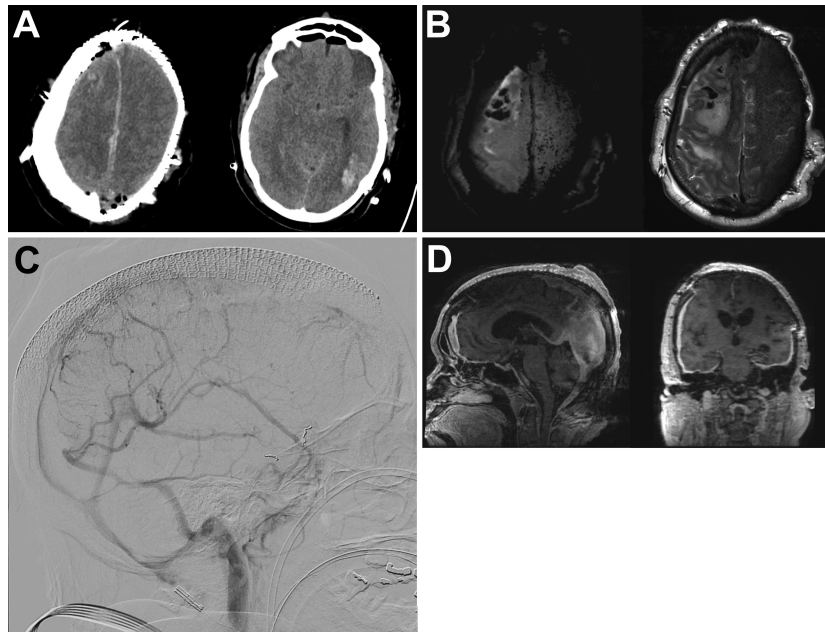


FIG. 4. Postoperative imaging. **A:** Immediate postoperative head CT showing right frontal and left occipital IPH. **B:** Axial diffusion-weighted imaging (*left*) and T2-weighted MRI (*right*) sequences showing cerebral edema from venous congestion. **C:** Postoperative angiogram demonstrating unchanged venous sinus flow compared to the preoperative baseline. **D:** Contrast MRI sequences showing radical subtotal resection and reconstruction of the cranial vault with mesh cranioplasty.

Nodules composed of only microfollicles were noted throughout the specimen, and sheets of necrosis were identified. Papillary architecture was not present. Immunohistochemical staining was performed, and the tumor was found to be CK7 positive, CK20 negative, TTF-1 positive, and thyroglobulin positive. These morphological and immunohistochemical profiles supported a diagnosis of metastatic carcinoma consistent with thyroid origin. The follicular architecture and relative paucity of pleomorphic irregular nuclei with nuclear grooves favored metastatic follicular thyroid carcinoma over papillary thyroid carcinoma.

Informed Consent

The necessary informed consent was obtained in this study.

Discussion

To the best of our knowledge, our case report describes the largest intraosseous, metastatic, follicular thyroid carcinoma to the dura. This study highlights the operative management of a giant, hypervascular, transcalvarial lesion that invaded the sagittal sinus and abutted eloquent motor cortex. Although rare, our case emphasizes the importance of including metastatic thyroid carcinoma among the differential diagnoses of hypervascular skull lesions with combined extracranial and intracranial expansion.

Metastatic Thyroid Carcinoma to the CNS

Differentiated thyroid carcinoma (DTC) typically has an excellent prognosis, with 10-year survival rates greater than 90%.¹ However, when distant metastases are diagnosed, 5-year survival rates decrease to 50%, and they are the main cause of disease-specific

mortality for patients with DTC.²⁻⁴ Given the paucity of metastatic DTC to the CNS in the literature, survival rates specific to this subgroup are unclear. In a retrospective study of outcomes and prognostic factors for DTC patients with cranial metastases, the median survival after the diagnosis of cranial metastases was 27 months. Skull metastases (hazard ratio [HR] 0.27) and resection (HR 0.13) were identified as independent prognostic factors for a better outcome.⁵ Another study found that the median survival time was 33 months after the diagnosis of intracranial metastasis.⁶

DTCs include papillary, follicular, and Hurthle cell subtypes. The majority of DTCs are papillary, which outnumber follicular and Hurthle cell cancers by factors of 7- and 25-fold, respectively.⁷ While only a minority of patients (4%–15%) develop metastases, most commonly involving the lung, bone, and lymph nodes, fewer than 5% of patients will develop metastases to other locations.^{8,9} In these rare DTC metastases, the ratio of papillary to follicular and Hurthle cell subtypes is decreased from 1.5- and 12-fold, respectively.¹⁰ Interestingly, subgroup analysis showed that dural metastases were predominantly follicular.¹⁰ One possible explanation is that follicular thyroid cancers tend to spread hematogenously, as opposed to papillary subtypes, which are more likely to spread via lymphatics.

Estimates of CNS metastases range between 0.3% and 1.5% of DTC cases.^{6,11} In a recent retrospective series of almost 4000 patients with metastatic DTC, 12 patients (12/3982 = 0.3%) had CNS involvement.¹² Metastatic DTC itself appears to be a significant risk factor for CNS involvement, as up to 18% of patients with distant metastases to other locations have coexisting CNS metastases.¹³ An autopsy series of patients with DTCs yielded up to 20% of CNS involvement,⁶ which can reflect CNS metastases as a late end-stage presentation of DTC disease.

Observations

Our case emphasizes the importance of considering metastatic DTC in the differential diagnosis for durally based, transcalvarial lesions, even in patients without disseminated DTC. A prior case study described a patient with a similar, albeit smaller, extracranial follicular thyroid carcinoma arising from the left frontal calvaria.¹⁴ This patient, however, had widespread systemic involvement representing the more typical presentation of end-stage disease.^{13,15} In our current study, however, the patient had no detectable systemic disease beyond the local thyroid tumor.

Lessons

Due to the tumor's large extracalvarial extension, adjacency to the motor cortex, and invasion into the posterior SSS, our case illustrates several key operative principles. First, careful study of the preoperative cerebral angiogram is necessary to assess sinus patency, and embolization of arterial feeders is helpful to minimize catastrophic intraoperative blood loss. Second, the extracranial portion of the tumor is circumferentially dissected from the galea until the normal bony calvaria is exposed prior to central tumor debulking. Third, a tailored piecemeal craniotomy was required due to extensive bony erosion from the tumor. Fourth, achieving a safe resection includes protecting the vein of Trolard and continuous motor mapping bilaterally. Fifth, although the patient eventually had a good functional recovery, her immediate postoperative condition could have been a consequence of resecting her anterior and middle SSS. Occlusion of the middle SSS on the preoperative angiogram and minimal flow upon direct intraoperative inspection of the SSS informed our decision to ligate the anterior and middle SSS. However, sacrifice of the SSS, particularly in large tumors, can lead to unpredictable venous dynamics, resulting in venous hypertension and associated sequelae (Fig. 4B). In retrospect, leaving residual tumor in the sinus for adjuvant treatment may have been a safer choice.

References

1. Links TP, van Tol KM, Jager PL, et al. Life expectancy in differentiated thyroid cancer: a novel approach to survival analysis. *Endocr Relat Cancer*. 2005;12(2):273-280.
2. Kitamura Y, Shimizu K, Nagahama M, et al. Immediate causes of death in thyroid carcinoma: clinicopathological analysis of 161 fatal cases. *J Clin Endocrinol Metab*. 1999;84(11):4043-4049.
3. Mihailovic JM, Stefanovic LJ, Malesevic MD, Erak MD, Tesanovic DD. Metastatic differentiated thyroid carcinoma: clinical management and outcome of disease in patients with initial and late distant metastases. *Nucl Med Commun*. 2009;30(7):558-564.
4. Leite AKN, Cavalheiro BG, Kulcsar MA, et al. Deaths related to differentiated thyroid cancer: a rare but real event. *Arch Endocrinol Metab*. 2017;61(3):222-227.
5. Hong YW, Lin JD, Yu MC, Hsu CC, Lin YS. Outcomes and prognostic factors in thyroid cancer patients with cranial metastases: a retrospective cohort study of 4,683 patients. *Int J Surg*. 2018;55:182-187.

6. Lee HS, Yoo H, Lee SH, Gwak HS, Shin SH. Clinical characteristics and follow-up of intracranial metastases from thyroid cancer. *Acta Neurochir*. 2015;157(12):2185-2194.
7. Hundahl SA, Fleming ID, Fremgen AM, Menck HR. A National Cancer Data Base report on 53,856 cases of thyroid carcinoma treated in the U.S., 1985-1995. *Cancer*. 1998;83(12):2638-2648.
8. Lee J, Soh EY. Differentiated thyroid carcinoma presenting with distant metastasis at initial diagnosis: clinical outcomes and prognostic factors. *Ann Surg*. 2010;251(1):114-119.
9. Sampson E, Brierley JD, Le LW, Rotstein L, Tsang RW. Clinical management and outcome of papillary and follicular (differentiated) thyroid cancer presenting with distant metastasis at diagnosis. *Cancer*. 2007;110(7):1451-1456.
10. Madani A, Jozaghi Y, Tabah R, How J, Mitmaker E. Rare metastases of well-differentiated thyroid cancers: a systematic review. *Ann Surg Oncol*. 2015;22(2):460-466.
11. Henriques de Figueiredo B, Godbert Y, Soubeyran I, et al. Brain metastases from thyroid carcinoma: a retrospective study of 21 patients. *Thyroid*. 2014;24(2):270-276.
12. Zunino A, Pitoia F, Faure E, et al. Unusual metastases from differentiated thyroid carcinoma: analysis of 36 cases. *Endocrine*. 2019;65(3):630-636.
13. Dinneen SF, Valimaki MJ, Bergstralh EJ, Goellner JR, Gorman CA, Hay ID. Distant metastases in papillary thyroid carcinoma: 100 cases observed at one institution during 5 decades. *J Clin Endocrinol Metab*. 1995;80(7):2041-2045.
14. Heery CR, Engelhard HH, Slavin KV, Michals EA, Villano JL. Unusual CNS presentation of thyroid cancer. *Clin Neurol Neurosurg*. 2012;114(7):1107-1109.
15. McConahey WM, Hay ID, Woolner LB, Van Heerden JA, Taylor WF. Papillary thyroid cancer treated at the Mayo Clinic, 1946 through 1970: initial manifestations, pathologic findings, therapy, and outcome. *Mayo Clinic Proc*. 1986;61(12):978-996.

Disclosures

The authors report no conflict of interest concerning the materials or methods used in this study or the findings specified in this paper.

Author Contributions

Conception and design: Tarapore, Lee, Raygor. Acquisition of data: Tarapore, Raygor, Nichols. Analysis and interpretation of data: Tarapore, Nichols. Drafting the article: Tarapore, Lee, Nichols. Critically revising the article: Tarapore, Lee, Raygor. Reviewed submitted version of manuscript: Tarapore, Lee, Raygor. Approved the final version of the manuscript on behalf of all authors: Tarapore.

Correspondence

Phiroz E. Tarapore: University of California, San Francisco, CA. phiroz.tarapore@ucsf.edu.